Energy Nexus 20 (2025) 100592

Contents lists available at ScienceDirect

Energy Nexus

journal homepage: www.elsevier.com/locate/nexus

Full Length Article

Toward integrated crop and building simulation for controlled environment agriculture using EnergyPlus

Gilbert Larochelle Martin [a], Danielle Monfet [b,*]

[a] Laboratory of Energy Technologies, Hydro-Quebec Research Institute, Shawinigan, Canada
[b] Department of construction engineering, École de technologie supérieure, Montreal, Canada

ARTICLE INFO

Dataset link: EnergyPlus lettuces-steady-state (Original data)

Keywords:
CEA
CEA-HD
BEM
BPS
EnergyPlus
TRNSYS

ABSTRACT

This paper presents an approach for integrating crop modelling into building performance simulation (BPS) of controlled environment agriculture (CEA) spaces. A comprehensive review of recent literature on CEA energy modelling using building performance simulation (BPS) software highlighted the need for such integrated capabilities. Leveraging EnergyPlus and the Python application programming interface (API), the proposed approach estimates the hygrothermal (sensible and latent) loads within CEA spaces by applying a fixed-point iteration root-finding algorithm based on the crop-level energy balance. The implementation was verified using data from the literature, enhancing the applicability of BPS tools for simulating the unique environmental conditions of CEA spaces.

1. Introduction

Controlled environment agriculture (CEA) is sparking new interest in commercial endeavours and the scientific community to maintain food sovereignty and mitigate the risks of globalised food supply chains. CEA is a crop production system isolated from the weather by some enclosure where the growing environment conditions (light, temperature, humidity, airflow speed, and CO_2) are controlled to enhance crop yield. This is accomplished through active energy systems, which add or remove heat from the production space using a predefined control strategy.

CEA production space types span multiple configurations, such as greenhouses (GH), building-integrated controlled environment agriculture (BI-CEA), and high-density controlled environment agriculture (CEA-HD) spaces, sometimes referred to as vertical or interior farms, container farms, plant factories, or indoor plant environments, as illustrated in Fig. 1.

Greenhouses have been studied extensively in the literature [28,41,65], while the research on BI-CEA spaces is gaining momentum [10]. BI-CEA spaces are generally more expensive and complex, but they offer energy efficiency potential due to the synergies possible between different types of spaces within the building [86]. CEA-HD can be defined as spaces where crops are stacked vertically, making it suitable for local production in any climate and dense urban areas. Industrial applications have been reported to require 6–8 MW of peak demand with annual consumption of up to 70,000 MWh, with even larger installations in the planning stages [44]. The electricity costs can represent 20 % [66] to 40 % [16] of the operating expenses of CEA-HD production spaces. In these installations, electric lighting can represent 55 % [2] to 80 % [16] of the total electricity consumption. Thus, CEA-HD spaces are typically exothermal spaces with significant cooling and dehumidifying loads.

One way to assess energy-related expenditures and energy efficiency potential is through modelling. The level of complexity when modelling CEA spaces can vary significantly, from simple energy balances [52] and 1D dynamic models, based on the perfectly stirred assumption with uniform air properties, to 3D computational fluid dynamics models [28]. Energy use in CEA spaces is driven by electric lighting and the operation of heating, ventilation, and air conditioning (HVAC) systems required to maintain controlled indoor conditions. Although external loads have some influence, internal loads, primarily from artificial lighting and crop heat exchanges, especially latent loads from transpiration, are dominant. As a result, HVAC energy demand is associated mainly with cooling and dehumidification processes, which are essential for

* Corresponding author.
E-mail addresses: larochellemartin.gilbert@hydroquebec.com (G. Larochelle Martin), danielle.monfet@etsmtl.ca (D. Monfet).

https://doi.org/10.1016/j.nexus.2025.100592
Received 14 April 2025; Received in revised form 2 October 2025; Accepted 17 November 2025
Available online 19 November 2025

dissipating heat from lighting and controlling humidity generated by crop transpiration. As such, accurate crop modelling is necessary to ensure reliable assessment of the energy performance of CEA spaces. A few interfaces have been proposed to assist in greenhouse analysis, such as virtual growers [47] and SimulSerre [50]. The proposed greenhouse models and interfaces in the literature cannot be easily used or adapted to analyse other CEA or non-CEA spaces (e.g., office, retail store) for BI-CEA applications. These tools also offer limited modelling options for heating, ventilation, and air conditioning (HVAC) systems, which restricts their applicability for the design and energy analysis of the HVAC systems in CEA spaces.

Conventional buildings exhibit significant variations in geometry, envelope, vocation, occupancy, HVAC systems, etc. Nevertheless, several software tools have been developed to assess their energy performance. For decades now, building performance simulation (BPS) or building energy modelling (BEM) tools [25,37,58,109,119] have been used to model building thermal loads, assess the energy performance of designs, promote the implementation of energy-efficient HVAC systems, and quantify demand response control sequences, etc. More than 200 tools are listed in the Building Energy Software Tools directory [36]. These tools have been leveraged since at least 2012 to assess CEA spaces' thermal and energy performances. Still, a crucial component of the energy and mass balances of CEA spaces – the crop-level energy balance – is not often inherently modelled in these tools.

Between 2012 and 2025, 95 papers related to energy modelling of CEA production space (greenhouses, plant factories, vertical farms, etc.) using BPS software tools (EnergyPlus, TRNSYS, etc.) were reviewed from the Scopus and Compendex databases (Table 1), where GH, CEA-HD, and iRTG referred to greenhouses, high-density controlled environment agriculture, and integrated rooftop greenhouse, respectively. Yet, among the reviewed papers that used a BPS software tool, 50 did not include crop transpiration as part of the CEA space energy model.

When a crop energy model was included, ten introduced a constant humidity gain with a fixed value regardless of the indoor conditions (Table 1). This is concerning because the crop energy balance significantly influences the space peak loads, and failing to model crops could result in improperly sized HVAC equipment, especially for CEA-HD spaces [31,111]. More importantly, crop heat exchanges are influenced by the size of the leaves, which represents an effective area for latent and sensible heat exchanges. These exchanges are influenced by the lighting intensities as well as the indoor air conditions [112,113]. Out of the reviewed papers, 41 of them incorporated some crop energy modelling, which included the use of empirical data [67,128], the TRNSYS pool model, and user-specific models such as those proposed by Bonachela et al. [26], Frankenstein and Koenig [46], Ishigami et al. [59], and Pieters and Deltour [93], as shown in Table 1. However, few have considered the influence that indoor air conditions have on the crop energy balance. As such, it was recommended to add vapour pressure deficit (VPD) calculation capabilities to BPS software tools [5].

Thus, the coupling of BPS software tools with CEA-related submodels has been investigated for over a decade [71]. The capabilities of these tools have been described extensively [37,38,119]. The two more commonly used tools for CEA energy modelling are TRNSYS and EnergyPlus: among the reviewed papers, 37 % used EnergyPlus, 54 % used TRNSYS, and 3 % used other tools (Table 1). TRNSYS is a more research-oriented commercial tool, where one can write and customise code relatively easily and leverage the solver for specific research needs. EnergyPlus is free software, but modifying or tailoring it to a particular modelling need can be more challenging. Basic routines can be added through an Energy Management System (EMS) routine using the EnergyPlus Runtime Language (ERL) language, and a Python API has been recently introduced. Although TRNSYS is flexible, customisable, and well-suited for research applications, co-simulation with EnergyPlus is valuable because it offers advanced and detailed modelling of building physics (e.g., heat transfer, HVAC systems, controls) that are not as easily implemented in TRNSYS. In addition, EnergyPlus is freely available and has become increasingly accessible through its EMS routines and Python API. A crop energy model was included in about 45 % of the cases for both tools (EnergyPlus and TRNSYS). Energy modelling of CEA-HD represents about 10 % of the reviewed papers. However, none of the modelled CEA-HD spaces in EnergyPlus included a fully integrated crop energy model that could be used under different growing conditions.

The reviewed literature highlights the need for improved modelling approaches that can accurately represent the diverse conditions and systems found in CEA spaces. More specifically, lighting and crops, the two main internal loads, must be adequately represented [113]. Crops absorb photosynthetically active radiation (PAR) emitted by the lighting, which drives photosynthesis and raises leaf surface temperatures. Simultaneously, transpiration releases water vapour through stomata, resulting in latent heat loss that cools the crops, which is influenced by indoor environmental conditions. Since lighting is both an energy input and a means to meet daily light integral requirements, representing crop heat exchanges with simple static terms cannot capture hourly feedback. Accurate modelling is therefore essential to reproduce the dynamic interactions between lighting, crops, and indoor environmental conditions maintained by HVAC systems. This can be addressed by coupling multiple tools to model and simulate specific systems and building concepts [22]. Effective CEA co-simulation requires key features such as runtime control, interactive data exchange, usability and ease of implementation. Among the most widely used BPS tools for CEA modelling, TRNSYS, built on a modular structure with a central solver, provides more flexibility, timestep control and straightforward data exchange between components. However, it can become computationally slower for large systems, particularly when numerous components are coupled together, as is often the case for CEA applications. In contrast, EnergyPlus supports variable exchange during runtime through external interfaces such as EMS and Python API, enabling direct scripting, runtime interaction, and efficient data access. Its integrated solver further enhances computational efficiency. Building on these strengths, this paper proposes an approach to support BPS of CEA spaces by integrating a crop energy balance model into the EnergyPlus building simulation software

Fig. 1. Different types of CEA spaces: (a) greenhouse (GH), (b) BI-CEA, and (c) CEA-HD.

Table 1
Examples of CEA space models in BPS software.

Crop Energy Models	BPS tool	Space type	References
No crop energy model	EnergyPlus	GH	Fabrizio [45]; Alvarez-Sánchez et al. [8]; Treethidtaphat et al. [118]; Zhang et al. [131]; Lee et al. [74]; Denzer et al. [42]; Gao et al. [49]; Thomas et al. [115]; Chen et al. [33]; Dahlan et al. [39]; Léveillé-Guillemette and Monfet [76]; Chen et al. [34]; Molina et al. [85]; Mohsenipour et al. [84]; Lebre et al. [69]; Jahangir et al. [60]; Kaliakatsos et al. [64]; Ma et al. [79]; Pakari and Ghani [91]; Tian et al. [116]
	TRNSYS	GH	Attar et al. [14]; Attar and Farhat [15]; Awani et al. [17]; Ha et al. [55]; Ataei [13]; Vadiee et al. [121]; Awani et al. [18]; Henshaw [57]; Jin et al. [62]; Rasheed et al. [96]; Yildirim and Bilir [129]; Rasheed et al. [97]; Asa'd et al. [11]; Rasheed et al. [98]; Pineda et al. [94]; Rasheed et al. [99]; Rasheed et al. [100]; Sayyah et al. [103]; Torres Pineda et al. [117]; Wang et al. [123]; Yang et al. [126]; Agrebi et al. [3]; Chahidi and Mechaqrane [32]; Mohammadi et al. [83]; Rasheed et al. [101]; Lee et al. [73]; Ogunlowo et al. [89]; Rabiu et al. [95]; Rasheed et al. [102]
	TRNSYS	CEA-HD	Yang et al. [127]
Constant humidity gain	EnergyPlus	GH	Harbick and Albright [56]; Dahlan et al. [40]
		GH & CEA-HD	Fuller et al. [48]
	TRNSYS	GH	Candy et al. [30]; Semple et al. [106]; Semple et al. [104,105] Vadiee and Martin [120]; Ahamed et al. [4]; Adesanya et al. [1]
FAO - Penman [92]	EnergyPlus	GH	Alinejad et al. [6]
		GH & CEA-HD	Liebman-Pelaez et al. [77]
		Living wall	Wang et al. [122].
	TRNSYS	GH	Baglivo et al. [19]; Mazzeo et al. [82]; Bonuso et al. [27]
		GH & CEA-HD	Zhang and Kacira [130]
Stanghellini [107]	EnergyPlus	GH	Benis et al. [24]
		iRTG	Ledesma et al. [70]
	TRNSYS	GH	Choab et al. [35]; Lee et al. [75]; Banakar et al. [23]
	Other	GH	Ward et al. [124]; Altes-Buch et al. [7]
Graamans et al. [52]	EnergyPlus	GH	Jans-Singh et al. [61]
		GH & CEA-HD	Graamans et al. [53]; Graamans et al. [54]
		CEA-HD	Eaton et al. [43]
	TRNSYS	CEA-HD	Lalonde et al. [68]; Talbot and Monfet [111]
Other	EnergyPlus	GH	Chahidi et al. [31]; Ouazzani Chahidi and Mechaqrane [90]
	EnergyPlus	iRTG	Nadal et al. [87]; Muñoz-Liesa et al. [86]
	TRNSYS	GH	Mashonjowa et al. [81]; Amin and Kissock [9]; Goto et al. [51]; Liu et al. [78]; Yeo et al. [128]; [67]
Unspecified	TRNSYS	GH	Bambara and Athienitis [20]; Bambara et al. [21]
	Other	GH	Lee et al. [72]

[37] via external coupling using the Python API. The integration of the crop energy model into EnergyPlus is verified using data available in the literature. The following sections present the proposed modelling method (Section 2) and the results of implementing the crop energy sub-model (Section 3), followed by a discussion (Section 4) and conclusion (Section 5).

2. Method: crop energy modelling in EnergyPlus

The reviewed literature revealed that the necessary level of detail to accurately represent the energy balance at the crop level in CEA spaces is limited in BPS software, particularly for EnergyPlus. This section details the modelling method developed to estimate the sensible and latent heat gain/loss induced by crops in the EnergyPlus software. This consists of two parts: (1) the algorithm used to solve the energy balance at the crop level and (2) its integration into EnergyPlus via the Python API.

2.1. Crop energy balance model

The crop-level energy balance can be represented using an energy balance at the leaf level [92] or detailed physiological growth models [29,63]. The model implemented in this study is based on the steady-state lettuce model proposed by Graamans et al. [52], which was experimentally validated under controlled conditions as part of a study of a controlled-environment agriculture (CEA) space. This crop energy model has also been previously integrated into TRNSYS, with the system of equations solved using the superlinear secant method [111]. In the present work, the same steady-state lettuce crop energy model is implemented in EnergyPlus to estimate the heat gain/loss induced by crops under varying indoor conditions, including lighting intensity, temperature, and humidity setpoints. To ensure proper integration within the existing simulation framework, the steady-state model was selected over the recently available dynamic crop model. In the steady-state model, the LAI remains fixed over time, while heat exchanges vary with lighting and indoor air conditions. In contrast, the dynamic model accounts for plant growth (with a varying LAI) together with lighting and indoor air conditions to estimate yield and heat exchanges, but requires a larger set of input parameters [113]. The energy balance is illustrated in Fig. 2 and defined by Eq. (1). Eq. (1) is formulated based on the assumptions proposed by Stanghellini [108], which consider the impact of longwave radiation ($q''_{LWX,plt}$) and thermal storage within the leaves and stems as being negligible [108]. This energy balance is computed at the leaf level. It includes three main terms: the net shortwave radiation absorbed by the plant surface ($q''_{SW,plt}$), the convective ($q''_{conv,plt}$) and the latent ($q''_{latent,plt}$) heat exchanges between the leaf and its environment as defined by Eqs. (2) to (4). Under the model assumptions, convective heat exchange is treated as a sensible heat gain or loss to the surrounding space.

$$q''_{SW,plt} - q''_{conv,plt} - q''_{latent,plt} = 0 \tag{1}$$

$$q''_{SW,plt} = (1-\rho_r)\cdot P_{el}\cdot f_v \cdot \mathrm{CAC} \tag{2}$$

$$q''_{conv,plt} = LAI\cdot\rho_a\cdot c_{p_a}\frac{T_{plt}-T_a}{r_a} \tag{3}$$

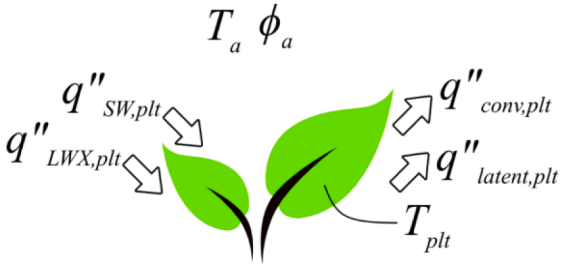

Fig. 2. Energy balance at the leaf level.
(Adapted from Talbot and Monfet [111])

$$q''_{latent,plt} = LAI \cdot \lambda \frac{\chi_s - \chi_a}{r_s + r_a} \quad (4)$$

where ρ_r is the reflection coefficient of the crop (-), P_{el} is the installed electric lighting power density (W·m^{-2}), f_v is the visible fraction (-), CAC is the cultivation area cover (-), *LAI* is the leaf area index (-), the total one-sided leaf area per horizontal surface unit [125], λ is the latent heat of vaporisation (kJ·kg^{-1}), χ_s and is χ_a are the vapour concentration at the leaf surface and of the indoor air (g·m^{-3}), r_s (s·m^{-1}) and r_a (s·m^{-1}) are the stomatal and aerodynamic resistances as defined by Eqs. (5) and (6) respectively, ρ_a is the indoor air density (kg·m^{-3}), c_{p_a} is the indoor air specific heat at constant pressure (kJ·kg^{-1}), T_{plt} is the leaf temperature (°C), T_a is the indoor air temperature (°C), and ϕ_a is the relative humidity (%). The formulations used for the stomatal and aerodynamic resistances are according to those reported by Graamans et al. [52] and Talbot and Monfet [111]. They are estimated solely as a function of the photosynthetic photon flux density and for forced convection conditions.

$$r_s = 60 \cdot \frac{(1500 + \mathrm{PPFD})}{(200 + \mathrm{PPFD})} \quad (5)$$

$$r_a = 100 \quad (6)$$

where PPFD is the photosynthetic photon flux density (μmol·s^{-1}·m^{-2}) and represents the number of photons in the 400–700 nm waveband incident per unit time on a unit surface. The 400–700 nm waveband is known as the photosynthetically active radiation (PAR) linked to the photosynthesis chemical process in the produced crops. The PPFD is used to compute the stomatal resistance and is estimated using the installed electric lighting power per unit area (P_{el}, W·m^{-2}) and the photosynthetic photon efficiency (PPE, μmol·J^{-1}) as described in Eq. (7). The proposed formulation implies that the crops intercept all the PAR emitted by the lighting fixtures.

$$\mathrm{PPFD} = P_{el} \cdot \mathrm{PPE} \quad (7)$$

The proposed model is programmed to be solved using a fixed-point iteration root-finding algorithm rather than the superlinear secant method, as implemented in the TRNSYS version of the model [111], for which convergence was not guaranteed. This modification improves code performance. Using fixed-point iteration implies writing the energy balance equation in the form described by Eq. (8), which has been shown to converge for $|g'(x)| < 1$ and where the rate of convergence is at least quadratic if $g'(r) = 0$, where r is the root.

$$x = g(x) \quad (8)$$

As illustrated in Fig. 3, the algorithm, the API while loop, is solved by first calculating the vapour concentration at the leaf surface (χ_s, g·m^{-3}) according to Eq. (9) for an initial leaf surface temperature (T_{plt}, °C) guess and indoor air conditions retrieved from the BPS software. The indoor air conditions are determined according to the indoor air temperature (T_a, °C), indoor air saturated vapour concentration (χ^*_a, g·m^{-3}), air density (ρ_a, kg·m^{-3}), air specific heat at constant pressure (c_p, kJ·kg^{-1}), the latent heat of vaporisation (λ, kJ·kg^{-1}), and the slope of the saturation function curve (ε, -). It is essential to mention that the indoor air saturated vapour concentration and the indoor air vapour concentration are not dependent on the leaf surface temperature.

$$\chi_s = \chi^*_a + \frac{\rho_a \cdot c_p \cdot \varepsilon}{\lambda} \cdot (T_{plt} - T_a) \quad (9)$$

Once the algorithm has solved for the vapour concentration at the leaf surface, the latent heat gain per surface area ($q''_{latent,plt}$, W·m^{-2}) is computed according to Eq. (4). Then, the convective (sensible) heat gain per surface area ($q''_{conv,plt}$, W·m^{-2}) is computed according to Eq. (3), using the net radiation, often referred to as R_{net} in the literature, which is equivalent to the short-wave radiation by electric lighting ($q''_{SW,plt}$, W·m^{-2}) presented in Eq. (2). A new leaf surface temperature is then estimated using Eq. (10).

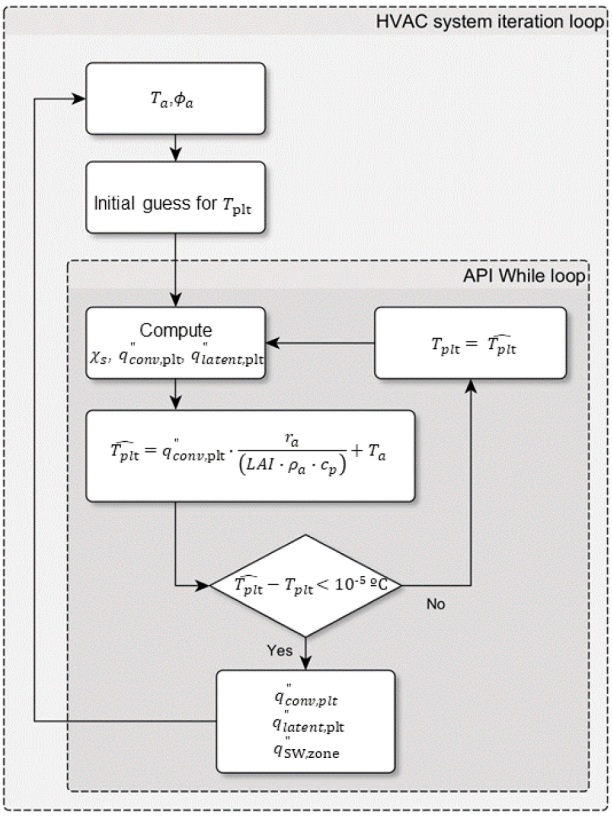

Fig. 3. Flowchart of the proposed fixed point iteration root-finding algorithm developed to solve the leaf level energy balance.

$$\widehat{T_{plt}} = q''_{conv,plt} \cdot \frac{r_a}{(LAI \cdot \rho_a \cdot c_p)} + T_a \quad (10)$$

The residual (*res*, °C) is computed using Eq. (11). On the next iteration, the leaf surface temperature (T_{pl}, °C) is replaced by the estimated leaf surface temperature ($\widehat{T_{pl}}$, °C) at the previous iteration and the algorithm is run again until the convergence criterion of 10^{-5} °C is met. During an annual simulation, the algorithm converged in 6 iterations for most of the timesteps (10 min). Once the API While loop is solved, the values obtained are used by the HVAC system iteration loop to determine the required capacities.

$$res = \widehat{T_{plt}} - T_{plt} \quad (11)$$

2.2. Implementation in EnergyPlus using an API

The EnergyPlus Python API is used to manage the data exchange between the crop energy balance and the thermal zone during the simulation run period using the «*on_begin_new_environment*» and the «*on_inside_hvac_system_iteration_loop*» EnergyPlus simulation calling points. The «*on_begin_new_environment*» is called only once during the simulation run time, and the «*on_inside_hvac_system_iteration_loop*» is called at least once every simulation timestep. Fig. 4 illustrates the proposed simulation process leveraging the EnergyPlus Python API and the energy balance at the crop level [52,111].

The weather file and building description represent the typical information needed to create a building energy model with building performance simulation (BPS) software. The parameters of the crop energy balance model, presented in Table 2, are stored in a separate file read before starting the simulation. The cultivated area cover (CAC),

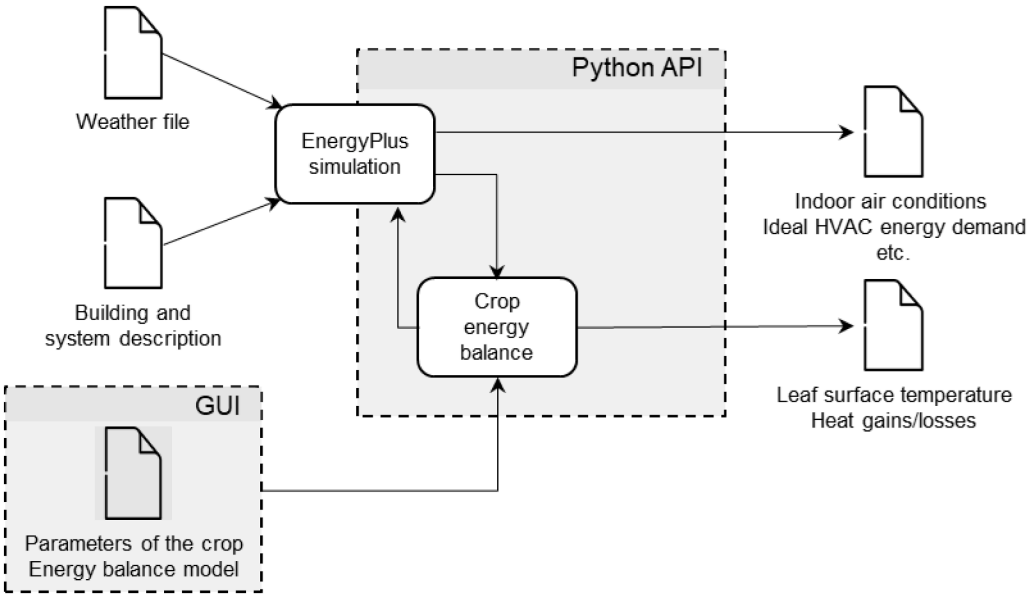

Fig. 4. Overview of the data exchange between EnergyPlus, the API and the crop energy balance model.

Table 2
Parameters of the crop energy balance model used by the API.

Software	Parameters	Units
GUI	Leaf area index (LAI)	dimensionless
	Cultivated Area	m^2
	Electric lighting power density (P_{el})	$W{\cdot}m^{-2}$
	Radiant Fraction (f_{LW})	dimensionless
	Visible Fraction (f_v)	dimensionless
	Photosynthetic photon efficiency (PPE)	$\mu mol{\cdot}J^{-1}$
	Reflection coefficient of the crop (ρ_r)	dimensionless
	Thermal Zone name	-
EnergyPlus	Lighting Level	W
	Photoperiod Schedule	boolean

estimated as being equal to 30.74 × LAI for LAI≤2.45 [114], and cultivated density (CD), defined as the sum of all the growing bed areas over the CEA space floor area, are derived from these inputs. The visible fraction (f_v) is the percentage of energy converted into shortwave radiation, the radiant fraction (f_{LW}) is the longwave radiation to the zone, and the balance is considered a convective gain.

The EnergyPlus simulation inputs, convective (sensible), and latent and radiative gains or losses, as illustrated in Fig. 3, are added to the thermal zone of the building model through the «*OtherEquipment*» objects and the specific Python plugin objects. The code used to solve the crop energy balance is programmed in Python, is publicly available, and has been verified through inter-software comparison and a case study, as shown in the results section (Section 3).

3. Results

The proposed coupling approach is evaluated through a two-stage verification process using data from the literature. First, the accuracy of the modified algorithm is assessed by comparing the computed leaf surface temperature and the associated sensible and latent heat fluxes against reference values. Second, the integrated model is applied to a case study of a small-scale high-density controlled environment agriculture (CEA-HD) space to compare peak load estimates and annual energy consumption, thereby assessing the impact of crop modelling on overall building performance simulation outcomes.

3.1. Leaf surface temperature and heat gains/losses

The first comparison verifies the implemented algorithm by focusing on the computed leaf surface temperature, where only the outputs of the crop energy model are investigated. The results from the EnergyPlus implementation—using a simplified box model with the ideal load option—are compared to those obtained from the open-access TRNSYS Type model. Both simulations apply the same crop-level energy balance equations and use the same weather file, ensuring identical conditions for evaluating the accuracy of the algorithm and its numerical behaviour.

The residuals between the leaf temperature simulated in TRNSYS and EnergyPlus are computed once steady-state conditions are reached in TRNSYS, i.e., with the first 20 first-time steps (200 min) excluded from the analysis. The maximum absolute difference (MAD) and the root mean square error (RMSE), defined according to Eqs. (12) and (13), are respectively 0.14 °C and 0.038 °C.

$$\mathrm{MAD} = max(|y_i - \hat{y}_i|),\ i = 1 \ldots n \tag{12}$$

$$\mathrm{RMSE} = \left[\frac{\sum_{i=1}^{n}(y_i - \hat{y}_i)^2}{n}\right]^{1/2} \tag{13}$$

where y_i is the TRNSYS reference value, $\hat{y}_i$ is the EnergyPlus estimated output value, and n the number of reference values.

Following this first comparison, the convective (sensible) and latent heat gains/losses induced by the crops are calculated, as summarised in Table 3. To assess the agreement between the TRNSYS and EnergyPlus results, the normalised mean bias error (NMBE) and the coefficient of

Table 3
Computed heat gain/loss from crop energy balance model in TRNSYS versus EnergyPlus.

Crop model output	TRNSYS		EnergyPlus		NMBE (%)	CV-RMSE (%)
	Lights off	Lights on	Lights off	Lights on		
Convective heat gain/loss (W)	−84.5	72.3	−84.9	72.4	0.04	0.7
Latent heat gain (W)	84.5	275.7	84.6	275.8	0.06	1.0

variation of the root mean square error (CV-RMSE) are computed using Eqs. (14) and (15). These two standard metrics, commonly used in building energy simulation to evaluate energy, demand and water savings [12], provide a basis for quantitative comparison. Notably, the radiative gains were identical in both models. The low values of the statistical indicators indicate good agreement and are considered satisfactory for algorithm verification.

$$\mathrm{CV-RMSE} = \left[\frac{\sum_{i=1}^{n}(y_i - \hat{y}_i)^2}{(n-p)}\right]^{1/2} \Big/ \bar{y} \times 100 \quad (14)$$

$$\mathrm{NMBE} = \frac{\sum_{i=1}^{n}(y_i - \hat{y}_i)}{(n-p)\times\bar{y}} \times 100 \quad (15)$$

3.2. Case study

As a second verification step, the peak demand and the annual energy consumption of a small-scale experimental high-density controlled environment agriculture (CEA-HD) space, located within a Montreal (QC) institutional building maintained at an ambient temperature of 20 °C, are computed using the EnergyPlus ideal loads option. This comparison assesses the impact of integrating the crop energy model on overall building performance metrics. This implies that only the loads were computed for the CEA space, with no detailed modelling of the heating, ventilation, and air conditioning (HVAC) system or specification of equipment capacities or performance data. The production system is a three-tier hydroponic nutrient film technique (NFT) system with a nutrient holding tank below and a light-emitting diode (LED) lighting system, as illustrated in Fig. 5. The production space has an envelope consisting of Structural Insulated Panels (SIPs), a foam core sandwiched between two oriented strand board (OSB) sheathings, having a thermal conductance of 0.12 $W\cdot(^{\circ}K\cdot m^2)^{-1}$, a thermal capacity of 100 $J\cdot(kg\cdot^{\circ}K)^{-1}$, and a density of 113.17 $kg\cdot m^{-3}$. During the photoperiod, which lasts for 16 h from 4:00 to 20:00, the space is maintained at a temperature of 21 °C and a relative humidity of 70 %. In comparison, it is being held at 18 °C with a 74 % relative humidity during the dark period (20:00 to 4:00). The installed electric lighting density is 144 $W\cdot m^{-2}$ of the cultivated area with a photosynthetic photon flux density (PPFD) of 288.5 $\mu mol\cdot s^{-1}\cdot m^{-2}$ (PPE of 2), a visible fraction (f_v) of 0.4 and a radiant fraction (f_{LW}) of 0.17. The LAI is estimated at 2.1, with a cultivated-to-footprint area ratio of 1.67.

As an initial verification step, the peak demands of the small-scale CEA-HD space are computed. In the absence of crops, the only internal heat gain is the sensible load from lighting, resulting in a peak dehumidification demand of zero. Under these conditions, the peak cooling and heating demands are 1290 kW and 50 kW, respectively. When crops are included, the peak demands are 778 kW for dehumidification, 1042 kW for cooling, and 250 kW for heating (Table 4). These changes reflect the effects of crop transpiration: as crops release moisture, the increased latent load drives dehumidification demand, while the lower leaf temperatures cool the surrounding air, resulting in a sensible heat loss that contributes to heating demand. The results obtained using the proposed modelling method in EnergyPlus, described in Section 2, are compared with those from an equivalent TRNSYS model published by Talbot et al. [110]. Table 4 presents the peak demand and the annual energy consumption for dehumidification, cooling, and heating by both models. In both cases, humidification is negligible. The results indicate that both models lead to values of the same order of magnitude, with minor discrepancies observed. To ensure a consistent comparison, two modelling scenarios were evaluated in EnergyPlus: one excluding crop-reflected shortwave radiation (EnergyPlus w/o radiation in Table 4), which yielded results closely aligned with the TRNSYS model, as reflected by the relative errors (R.E.%) presented in Table 4, and a second scenario incorporating the crop-reflected shortwave radiation (EnergyPlus w/radiation in Table 4). This modification does not affect latent heat exchange or dehumidification demand, as the PAR available for photosynthesis remains unchanged. However, it does

Table 4
TRNSYS and EnergyPlus "ideal" peak demand and annual energy consumption for a CEA-HD space.

		TRNSYS	EnergyPlus		
		w/o radiation	w/o radiation	R. E. (%)	w/ radiation
Dehumidification	Peak demand (W)	725	778	7.3	778
	Consumption (kWh)	4323	4371	1.1	4371
Cooling	Peak demand (W)	932	934	0.2	1042
	Consumption (kWh)	5415	5419	0.1	6045
Heating	Peak demand (W)	247	250	1.2	250
	Consumption (kWh)	693	698	0.7	696

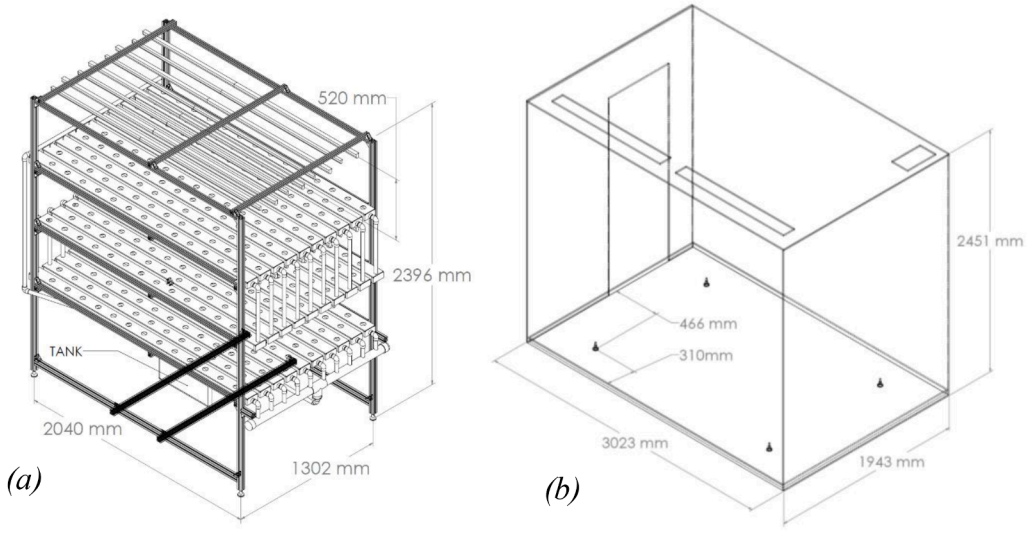

Fig. 5. Schematics of (a) the production system and (b) the enclosure.

influence sensible cooling by increasing heat gains to the space when crop-reflected shortwave radiation is accounted for. Therefore, including radiation improves the representation of crop energy balance and more accurately captures the heat exchanges driving sensible cooling compared to the model without radiation.

Minor differences between the two software are expected due to different modelling assumptions, such as, for example, the radiative model or application of adiabatic boundary conditions (see Magni et al. [80]). Nonetheless, the results fall well within acceptable bounds, exceeding the benchmarking accuracy reported by BESTEST results. The BESTEST (Building Energy Simulation Test) is a standardised validation procedure for building energy simulation software, which evaluates performance across a series of test cases involving different building configurations. According to Neymark et al. [88], typical discrepancies in BESTEST are around 20 % in peak cooling demand and 15 % for annual cooling energy. In contrast, the current study showed much lower deviations. Furthermore, a visual inspection of the heat exchange rates, including room air temperature, relative humidity, and leaf temperature of the crop, revealed nearly identical profiles between the TRNSYS and EnergyPlus models, further validating the approach.

Modelling the crop energy balance remains a complex task for most building performance simulation practitioners due to the detailed biophysical processes involved and the limitations of existing tools. An open-access implementation has been developed to streamline integration into EnergyPlus workflows to support the broader adoption of the proposed modelling approach. This implementation automates the generation of required model parameters (as described in Table 2), simplifying the inclusion of CEA production space models within existing thermal zone configurations. The tool is available on GitHub (https://github.com/ltsb-etsmtl) to facilitate future research, replication, and practical application.

4. Discussion

The proposed crop-level energy model integration into EnergyPlus addresses a gap in the literature by offering sufficient detail for replicable implementation using the EnergyPlus API. This work outlines a detailed and referenced process to model CEA spaces, including the heat gain/loss induced by crops, within a free, supported, publicly available, and validated BPS software, EnergyPlus. While the implementation has been verified through comparison with published models, further validation using real-world case studies is necessary. Such data would offer valuable feedback for refining the crop energy model and informing future tool developments. The proposed GUI is a basic version of a laboratory research tool designed to adapt and evolve based on users' needs and feedback. Limitations of the current implementation of the crop energy model include simplified assumptions related to the lighting systems, the absence of crop growth, cultivar specificity, and the lack of consideration for abiotic stress metrics. These limitations will be addressed in future work by adapting the proposed crop model to align with the more advanced one developed by Talbot and Monfet [113]. Nonetheless, this incremental advancement represents a meaningful step towards achieving a more comprehensive modelling of CEA spaces by leveraging decades of energy-related research embedded within BPS software. The adaptable approach could be extended to other types of CEA environments, such as greenhouses or other types of crops. Implementing the model for different crop types can be easily achieved by adjusting the input variables, such as the LAI, lighting intensity and duration, and indoor air conditions, and modifying model parameters, including the reflection coefficient, stomatal resistance, and aerodynamic resistance, based on values available in the literature for each specific crop.

5. Conclusion

The literature review highlighted the limited capability of current BPS software to model crop energy balances effectively. This paper proposed a publicly available method to integrate a crop-level energy model into EnergyPlus using its Python application programming interface (API). The method relies on a fixed-point iteration root-finding algorithm to solve the crop energy balance and was verified against results from a published TRNSYS model and a case study. By extending EnergyPlus with this modelling capability, the approach provides new opportunities for accurately designing, operating, and optimising CEA environments in building simulation research and HVAC system development.

CRediT authorship contribution statement

Gilbert Larochelle Martin: Writing – original draft, Methodology, Formal analysis, Conceptualization. **Danielle Monfet:** Writing – review & editing, Supervision, Project administration, Conceptualization.

Declaration of competing interest

The authors declare the following financial interests/personal relationships which may be considered as potential competing interests: Gilbert Larochelle Martin reports financial support was provided by Fonds de recherche du Québec - Nature et technologies. If there are other authors, they declare that they have no known competing financial interests or personal relationships that could have appeared to influence the work reported in this paper.

Data availability

A link to the model is included within the article.
EnergyPlus lettuces-steady-state (Original data) (GitHub)

References

[1] M.A. Adesanya, W.-H. Na, A. Rabiu, et al., TRNSYS simulation and experimental validation of internal temperature and heating demand in a glass greenhouse, Sustainability 14 (2022) 8283.
[2] Agritecture, Global CEA Census Report 2021. https://www.agritecture.com/census, 2021.
[3] S. Agrebi, R. Chargui, B. Tashtoush, et al., Comparative performance analysis of a solar assisted heat pump for greenhouse heating in Tunisia, Int. J. Refrig. 131 (2021) 547–558.
[4] M.S. Ahamed, H. Guo, K. Tanino, Modeling heating demands in a Chinese-style solar greenhouse using the transient building energy simulation model TRNSYS, J. Build. Eng. 29 (2020) 101114.
[5] T. Akpenpuun, Q. Ogunlowo, A. Rabiu, et al., Building Energy Simulation model application to greenhouse microclimate, covering material and thermal blanket modelling: a review, Niger. J. Technol. Dev. 19 (2022) 276–286.
[6] T. Alinejad, M. Yaghoubi, A. Vadiee, Thermo-environomic assessment of an integrated greenhouse with an adjustable solar photovoltaic blind system, Renew. Energy 156 (2020) 1–13.
[7] Q. Altes-Buch, S. Quoilin, V. Lemort, A modeling framework for the integration of electrical and thermal energy systems in greenhouses, Build. Simul. 15 (2022) 779–797.
[8] E. Alvarez-Sánchez, G. Leyva-Retureta, E. Portilla-Flores, et al., Evaluation of thermal behavior for an asymmetric greenhouse by means of dynamic simulations, Dyna (Medellin) 81 (2014) 152–159.
[9] M.T. Amin, J.K. Kissock, Dynamic modeling and verification of an energy-efficient greenhouse with aquaponics, Energy Sustainability (2016) V001T011A005.
[10] E. Appolloni, F. Orsini, K. Specht, et al., The global rise of urban rooftop agriculture: a review of worldwide cases, J. Clean. Prod. 296 (2021) 126556.
[11] O. Asa'd, V.I. Ugursal, N. Ben-Abdallah, Investigation of the energetic performance of an attached solar greenhouse through monitoring and simulation, Energy Sustain. Dev. 53 (2019) 15–29.
[12] ASHRAE (2014). Guideline 14-2014: measurement of energy, demand, and water savings. 1–150.
[13] A. Ataei, Performance optimization of a combined solar collector, geothermal heat pump and thermal seasonal storage system for heating and cooling greenhouses, J. Appl. Eng. Sci. 14 (2016) 296–305.
[14] I. Attar, N. Naili, N. Khalifa, et al., Parametric and numerical study of a solar system for heating a greenhouse equipped with a buried exchanger, Energy Convers. Manag. 70 (2013) 163–173.

[15] I. Attar, A. Farhat, Efficiency evaluation of a solar water heating system applied to the greenhouse climate, Sol. Energy 119 (2015) 212–224.
[16] D.D. Avgoustaki, G. Xydis, Energy cost reduction by shifting electricity demand in indoor vertical farms with artificial lighting, Biosyst. Eng. 211 (2021) 219–229.
[17] S. Awani, R. Chargui, S. Kooli, et al., Performance of the coupling of the flat plate collector and a heat pump system associated with a vertical heat exchanger for heating of the two types of greenhouses system, Energy Convers. Manag. 103 (2015) 266–275.
[18] S. Awani, S. Kooli, R. Chargui, et al., Numerical and experimental study of a closed loop for ground heat exchanger coupled with heat pump system and a solar collector for heating a glass greenhouse in north of Tunisia, Int. J. Refrig. 76 (2017) 328–341.
[19] C. Baglivo, D. Mazzeo, S. Panico, et al., Complete greenhouse dynamic simulation tool to assess the crop thermal well-being and energy needs, Appl. Therm. Eng. 179 (2020) 115698.
[20] J. Bambara, A.K. Athienitis, Energy and economic analysis for greenhouse ground insulation design, Energies 11 (2018).
[21] J. Bambara, A.K. Athienitis, U. Eicker, Decarbonizing local mobility and greenhouse agriculture through residential building energy upgrades: a case study for Québec, Energies 14 (2021).
[22] I. Beausoleil-Morrison, F. Macdonald, M. Kummert, et al., Co-simulation between ESP-r and TRNSYS, J. Build. Perform. Simul. 7 (2014) 133–151.
[23] A. Banakar, M. Montazeri, B. Ghobadian, et al., Energy analysis and assessing heating and cooling demands of closed greenhouse in Iran, Therm. Sci. Eng. Prog. 25 (2021) 101042.
[24] K. Benis, C. Reinhart, P. Ferrão, Development of a simulation-based decision support workflow for the implementation of Building-Integrated Agriculture (BIA) in urban contexts, J. Clean. Prod. 147 (2017) 589–602.
[25] B. Birdsall, W. Buhl, K. Ellington, et al., Overview of the DOE-2 Building Energy Analysis Program, Lawrence Berkeley Laboratory, Berkeley, CA, 1990. Report LBL-19735m rev. w.
[26] S. Bonachela, A.M. González, M.D. Fernández, Irrigation scheduling of plastic greenhouse vegetable crops based on historical weather data, Irrig. Sci. 25 (2006) 53–62.
[27] S. Bonuso, S. Panico, C. Baglivo, et al., Dynamic analysis of the natural and mechanical ventilation of a solar greenhouse by coupling controlled mechanical ventilation (CMV) with an earth-to-air heat exchanger (EAHX), Energies 13 (2020) 3676.
[28] T. Boulard, J.-C. Roy, J.-B. Pouillard, et al., Modelling of micrometeorology, canopy transpiration and photosynthesis in a closed greenhouse using computational fluid dynamics, Biosyst. Eng. 158 (2017) 110–133.
[29] N. Brisson, C. Gary, E. Justes, et al., An overview of the crop model STICS, Eur. J. Agron. 18 (2003) 309–332.
[30] S. Candy, G. Moore, P. Freere, Design and modeling of a greenhouse for a remote region in Nepal, Proc. Eng. (2012) 152–160.
[31] L.O. Chahidi, M. Fossa, A. Priarone, et al., Energy saving strategies in sustainable greenhouse cultivation in the mediterranean climate–A case study, Appl. Energy 282 (2021) 116156.
[32] L.O. Chahidi, A. Mechaqrane, Energetic and economic analysis for improving greenhouse energy efficiency, J. Energy Syst. 5 (2021) 296–305.
[33] C. Chen, Y. Li, N. Li, et al., A computational model to determine the optimal orientation for solar greenhouses located at different latitudes in China, Sol. Energy 165 (2018) 19–26.
[34] C. Chen, N. Yu, F. Yang, et al., Theoretical and experimental study on selection of physical dimensions of passive solar greenhouses for enhanced energy performance, Sol. Energy 191 (2019) 46–56.
[35] N. Choab, A. Allouhi, A. El Maakoul, et al., Effect of greenhouse design parameters on the heating and cooling requirement of greenhouses in Moroccan climatic conditions, IEEE Access 9 (2020) 2986–3003.
[36] D.B. Crawley, Building energy tools directory, Proc. Build. Simul.'97 1 (1997) 63–64.
[37] D.B. Crawley, L.K. Lawrie, F.C. Winkelmann, et al., EnergyPlus: creating a new-generation building energy simulation program, Energy Build. 33 (2001) 319–331.
[38] D.B. Crawley, J.W. Hand, M. Kummert, et al., Contrasting the capabilities of building energy performance simulation programs, Build Env. 43 (2008) 661–673.
[39] N. Dahlan, S. Sakimin, M. Faizwan, et al., Automated calibration of greenhouse energy model using hybrid evolutionary programming (EP)-energy Plus, Indones. J. Electr. Eng. Comput. Sci. 12 (2018) 648–654.
[40] N. Dahlan, A. Amiruddin, N.D. Luong, et al., Energy and climate analysis of greenhouse system for tomatoes cultivation using CFD and Open Studio Energy Plus software, Int. J. Eng. Technol. 7 (2018) 183–186.
[41] J. Deltour, D. De Halleux, J. Nijskens, et al., Dynamic modelling of heat and mass transfer in greenhouses, Symp. Greenh. Clim. Control 174 (1985) 119–126.
[42] A. Denzer, L. Wang, Y. Thomas, et al., Greenhouse design with waste heat: principles and practices, in: AEI 2017, 2017, pp. 440–455.
[43] M. Eaton, T. Shelford, M. Cole, et al., Modeling resource consumption and carbon emissions associated with lettuce production in plant factories, J. Clean. Prod. 384 (2023) 135569.
[44] EPRI, Indoor Agriculture: a Utility, Water, Sustainability, Technology and Market Overview, Electric Power Research Institute, 2018, p. 24.
[45] E. Fabrizio, Energy reduction measures in agricultural greenhouses heating: envelope, systems and solar energy collection, Energy Build. 53 (2012) 57–63.
[46] S. Frankenstein, G. Koenig, FASST Vegetation Models, Engineer Research and Development Center Hanover Nh Cold Regions Research, 2004.
[47] J.M. Frantz, B. Hand, L. Buckingham, et al., Virtual grower: software to calculate heating costs of greenhouse production in the United States, HortTechnology 20 (2010) 778–785.
[48] R.J. Fuller, L. Aye, A. Zahnd, et al., Thermal evaluation of a greenhouse in a remote high altitude area of Nepal, Int. Energy J. 10 (2009).
[49] X. Gao, H. Yang, Y. Guan, et al., Length determination of the solar greenhouse north wall in Lanzhou, Proce. Eng. (2017) 1230–1236.
[50] C. Gary, M. Tchamitchian, N. Bertin, et al., Simulserre: an Educational Software Simulating the Greenhouse-Crop System, 456 ed., International Society for Horticultural Science (ISHS), Leuven, Belgium, 1998, pp. 451–458.
[51] E. Goto, Y. Ishigami, L. Okushima, Development of a greenhouse simulation model to estimate energy and resources necessary for environmental controls under various climate conditions, Acta Hortic. (2017) 293–300.
[52] L. Graamans, A. van den Dobbelsteen, E. Meinen, et al., Plant factories; crop transpiration and energy balance, Agric. Syst. 153 (2017) 138–147.
[53] L. Graamans, E. Baeza, A. van den Dobbelsteen, et al., Plant factories versus greenhouses: comparison of resource use efficiency, Agric. Syst. 160 (2018) 31–43.
[54] L. Graamans, M. Tenpierik, A. van den Dobbelsteen, et al., Plant factories: reducing energy demand at high internal heat loads through facade design, Appl. Energy 262 (2020) 114544.
[55] T. Ha, I-b Lee, K-s Kwon, et al., Computation and field experiment validation of greenhouse energy load using building energy simulation model, Int. J. Agric. Biol. Eng. 8 (2015) 116–127.
[56] K. Harbick, L.D. Albright, Comparison of energy consumption: greenhouses and plant factories, Acta Hortic. 1134 (2016) 285–292.
[57] P. Henshaw, Modelling changes to an unheated greenhouse in the Canadian subarctic to lengthen the growing season, Sustain. Energy Technol. Assess. 24 (2017) 31–38.
[58] D. Herron, G. Walton, L. Lawrie, Building Loads analysis and System thermodynamics (BLAST) Program Users Manual. Volume one. Supplement (Version 3.0), Constr. Eng. Res. Lab (ARMY) CHAMPAIGN IL (1981).
[59] Y. Ishigami, E. Goto, M. Watanabe, et al., Development of a simulation model to evaluate environmental controls in a tomato greenhouse, Int. Symp. New Technol. Environ. Control Energy-Sav. Crop Prod. Greenh. Plant 1037 (2013) 93–98.
[60] M.H. Jahangir, M. Ziyaei, A. Kargarzadeh, Evaluation of thermal behavior and life cycle cost analysis of greenhouses with bio-phase change materials in multiple locations, J. Energy Storage 54 (2022) 105176.
[61] M. Jans-Singh, R. Ward, R. Choudhary, Co-simulating a greenhouse in a building to quantify co-benefits of different coupled configurations, J. Build. Perform. Simul. 14 (2021) 247–276.
[62] T.-H. Jin, K.-Y. Shin, S.-W. Yoon, et al., Simulation of thermal environment in a three-layer vinyl greenhouse by natural ventilation control, in: E3S Web of Conferences, EDP Sciences, 2017 00073.
[63] J.W. Jones, E. Dayan, L. Allen, et al., A dynamic tomato growth and yield model (TOMGRO), Trans. ASAE 34 (1991) 663–0672.
[64] D. Kaliakatsos, F. Nicoletti, F. Paradisi, et al., Evaluation of building energy savings achievable with an attached bioclimatic greenhouse: parametric analysis and solar gain control techniques, Buildings 12 (2022).
[65] B.A. Kimball, Simulation of the energy balance of a greenhouse, Agric. Meteorol. 11 (1973) 243–260.
[66] T. Kozai, G. Niu, M. Takagaki, Plant Factory: an Indoor Vertical Farming System for Efficient Quality Food Production, Academic press, 2019.
[67] Labihi A., Meslem A., Collet F., et al. Transient thermal simulation of a greenhouse for tomato plants: a Trnsys model with experimental validation. Prepr. submitt. 2023.
[68] T. Lalonde, M.H. Talbot, D. Monfet, The impacts of plants on HVAC system performances: a parametric study, in: Proceedings of Building Simulation 2019: 16th Conference of International Building Performance Simulation Association, 2019, pp. 1921–1928.
[69] B. Lebre, P.D. Silva, L.C. Pires, et al., Computational modeling of the thermal behavior of a greenhouse, Appl. Sci. 11 (2021) 11816.
[70] G. Ledesma, J. Nikolic, O. Pons-Valladares, Co-simulation for thermodynamic coupling of crops in buildings. Case study of free-running schools in Quito, Ecuador, Build. Env. 207 (2022) 108407.
[71] C. Lee, D. Costola, G. Swinkels, et al., On the use of building energy simulation programs in the performance assessment of agricultural greenhouses, in: Proceedings of the 1st Asia Conference of the International Building Performance Simulation Association, Shanghai, China, 2012, pp. 1–8.
[72] C. Lee, D. Cóstola, R. Loonen, et al., Energy saving potential of long-term climate adaptive greenhouse shells, in: Proceedings of Building Simulation 2013: 13th Conference of International Building Performance Simulation Association, 2013, pp. 954–961.
[73] C.-G. Lee, L-H Cho, S.-J. Kim, et al., Prediction model for the internal temperature of a greenhouse with a water-to-water heat pump using a pellet boiler as a heat source using building energy simulation, Energies 15 (2022) 5677.
[74] K.H. Lee, J.H. Lee, K.H. Lee, et al., Energetic and economic feasibility analysis of utilizing waste heat from incineration facility and power plant for large-scale horticulture facilities, Appl. Therm. Eng. 105 (2016) 577–593.
[75] S-Y Lee, I-B Lee, S-N Lee, et al., Dynamic energy exchange modelling for a plastic-covered multi-span greenhouse utilizing a thermal effluent from power plant, Agronomy 11 (2021) 1461.
[76] Léveillé-Guillemette F., Monfet D. (2018). Calibration d'un modèle énergétique et analyse économique de mesures de conservation d'énergie d'une serre communautaire à Montréal.

[77] M. Liebman-Pelaez, J. Kongoletos, L.K. Norford, et al., Validation of a building energy model of a hydroponic container farm and its application in urban design, Energy Build. 250 (2021) 111192.
[78] J. Liu, T.-H. Jin, K.-Y. Shin, Parametric study on a simplified model for the estimation of the heating and the cooling loads of a closed-span greenhouse: a case study in Korea, J. Mech. Sci. Technol. 35 (2021) 333–341.
[79] J. Ma, X. Du, S. Meng, et al., Simulation of thermal performance in a typical Chinese solar greenhouse, Agronomy 12 (2022).
[80] M. Magni, F. Ochs, S. de Vries, et al., Detailed cross comparison of building energy simulation tools results using a reference office building as a case study, Energy Build. 250 (2021) 111260.
[81] E. Mashonjowa, F. Ronsse, J.R. Milford, et al., Modelling the thermal performance of a naturally ventilated greenhouse in Zimbabwe using a dynamic greenhouse climate model, Sol. Energy 91 (2013) 381–393.
[82] D. Mazzeo, C. Baglivo, S. Panico, et al., Solar greenhouses: climates, glass selection, and plant well-being, Sol. Energy 230 (2021) 222–241.
[83] S. Mohammadi, E. Khalife, M. Kaveh, et al., Comparison of optimized and conventional models of passive solar greenhouse—case study: the indoor air temperature, irradiation, and energy demand, Energies 14 (2021) 5369.
[84] M. Mohsenipour, M. Ebadollahi, H. Rostamzadeh, et al., Design and evaluation of a solar-based trigeneration system for a nearly zero energy greenhouse in arid region, J. Clean. Prod. 254 (2020) 119990.
[85] J. Molina, M. Ponce, M. Horn, et al., Towards a sustainable bioclimatic approach for the Peruvian high Andean rural area: evaluation of the thermal contribution of a greenhouse attached to a dwelling, in: Proceedings of the International Solar Energy Society (ISES) Solar World Congress 2019 (SWC 2019) and the International Energy Agency (IEA) Solar Heating and Cooling (SHC) International Conference 2019, 2019, pp. 355–364.
[86] J. Muñoz-Liesa, M. Royapoor, E. Cuerva, et al., Building-integrated greenhouses raise energy co-benefits through active ventilation systems, Build. Env. 208 (2022) 108585.
[87] A. Nadal, P. Llorach-Massana, E. Cuerva, et al., Building-integrated rooftop greenhouses: an energy and environmental assessment in the mediterranean context, Appl. Energy 187 (2017) 338–351.
[88] J. Neymark, R. Judkoff, M. Kummert, et al., Update of ASHRAE Standard 140 Section 5.2 and Related Sections (BESTEST Building Thermal Fabric Test Cases), Argonne National Lab.(ANL), Argonne, ILUnited States, 2020.
[89] Q.O. Ogunlowo, W.H. Na, A. Rabiu, et al., Effect of envelope characteristics on the accuracy of discretised greenhouse model in TRNSYS, J. Agric. Eng. 53 (2022).
[90] L. Ouazzani Chahidi, A. Mechaqrane, Greenhouse Design Selection in Moroccan Climatic Conditions. *WITS 2020*, Springer, 2022, pp. 639–648.
[91] A. Pakari, S. Ghani, Regression equation for estimating the maximum cooling load of a greenhouse, Sol. Energy 237 (2022) 231–238.
[92] H.L. Penman, Natural evaporation from open water, bare soil and grass, Proc. R. Soc. Lond., A. Math. Phys. Sci. 193 (1948) 120–145.
[93] J.G. Pieters, J.M. Deltour, Performances of greenhouses with the presence of condensation on cladding materials, J. Agric. Eng. Res. 68 (1997) 125–137.
[94] I.T. Pineda, Y.D. Lee, J. Cho, et al., Environmental impacts of heating in a conventional greenhouse and a rooftop greenhouse for fresh tomato production, in: *ECOS 2020 - Proceedings of the 33rd International Conference on Efficiency, Cost, Optimization, Simulation and Environmental Impact of Energy Systems*, 2020, pp. 2318–2327.
[95] A. Rabiu, W.-H. Na, T.D. Akpenpuun, et al., Determination of overall heat transfer coefficient for greenhouse energy-saving screen using Trnsys and hotbox, Biosyst. Eng. 217 (2022) 83–101.
[96] A. Rasheed, J.W. Lee, H.W. Lee, Development of a model to calculate the overall heat transfer coefficient of greenhouse covers, Span. J. Agric. Res. 15 (2017).
[97] A. Rasheed, J.W. Lee, H.W. Lee, Development and optimization of a building energy simulation model to study the effect of greenhouse design parameters, Energies 11 (2018) 2001.
[98] A. Rasheed, W.H. Na, J.W. Lee, et al., Optimization of greenhouse thermal screens for maximized energy conservation, Energies 12 (2019) 3592.
[99] A. Rasheed, C.S. Kwak, W.H. Na, et al., Development of a building energy simulation model for control of multi-span greenhouse microclimate, Agronomy 10 (2020) 1236.
[100] A. Rasheed, C.S. Kwak, H.T. Kim, et al., Building energy and simulation model for analyzing energy saving options of multi-span greenhouses, Appl. Sci. 10 (2020) 6884.
[101] A. Rasheed, W.H. Na, J.W. Lee, et al., Development and validation of air-to-water heat pump model for greenhouse heating, Energies 14 (2021) 4714.
[102] A. Rasheed, H.T. Kim, H.W. Lee, Modeling-based energy performance assessment and validation of air-to-water heat pump system integrated with multi-span greenhouse on cooling mode, Agronomy 12 (2022) 1374.
[103] A.H.A. Sayyah, S. Mohammadi, A.M. Nikbakht, et al., Modeling and design a special type of passive solar greenhouse in cold climate by TRNSYS, J. Agric. Sci. 26 (2020) 488–498.
[104] L. Semple, R. Carriveau, D.S.K. Ting, A techno-economic analysis of seasonal thermal energy storage for greenhouse applications, Energy Build. 154 (2017) 175–187.
[105] L. Semple, R. Carriveau, D.S.K. Ting, Assessing heating and cooling demands of closed greenhouse systems in a cold climate, Int. J. Energy Res. 41 (2017) 1903–1913.
[106] L.M. Semple, R. Carriveau, D.S.K. Ting, Potential for large-scale solar collector system to offset carbon-based heating in the Ontario greenhouse sector, Int. J. Sustain. Energy 37 (2018) 378–392.
[107] C. Stanghellini, Transpiration of Greenhouse Crops: an Aid to Climate Management, Wageningen University and Research, 1987.
[108] C. Stanghellini, Transpiration of greenhouse crops. An Aid to Climate Management, IMAG, 1987.
[109] P. Strachan, G. Kokogiannakis, I. Macdonald, History and development of validation with the ESP-r simulation program, Build. Env. 43 (2008) 601–609.
[110] M.-H. Talbot, D. Monfet, T. Lalonde, et al., Impact of modelling thermal phenomena in a high-density controlled environment agriculture (CEA-HD) space, in: Proceedings of Building Simulation 2021: 17th Conference of IBPSA, IBPSA, 2021, pp. 1357–1364.
[111] M.-H. Talbot, D. Monfet, Estimating the impact of crops on peak loads of a building-integrated agriculture space, Sci. Technol. Built Environ. 26 (2020) 1448–1460.
[112] M.H. Talbot, D. Monfet, Development of a crop growth model for the energy analysis of controlled agriculture environment spaces, Biosyst. Eng. 238 (2024) 38–50.
[113] M.-H. Talbot, D. Monfet, Analysing the influence of growing conditions on both energy load and crop yield of a controlled environment agriculture space, Appl. Energy 368 (2024) 123406.
[114] F. Tei, A. Scaife, D.P. Aikman, Growth of lettuce, onion, and red beet. 1. Growth analysis, light interception, and radiation use efficiency, Ann. Bot. 78 (1996) 633–643.
[115] Y. Thomas, L. Wang, A. Denzer, Energy savings analysis of a greenhouse heated by waste heat, in: Building Simulation Conference Proceedings, 2017, pp. 1942–1947.
[116] C. Tian, Z. Shao, R. Wang, et al., Optimal design of integrated energy supply system for continuous greenhouse effect: a study on carbon emission and operational cost, in: Planning and Operation of Hybrid Renewable Energy Systems, 2022 845637128.
[117] I. Torres Pineda, J.H. Cho, D. Lee, et al., Environmental impact of fresh tomato production in an urban rooftop greenhouse in a humid continental climate in South Korea, Sustainability 12 (2020) 9029.
[118] W. Treethidtaphat, S. Kittipiyakul, K. Kaemarungsi, et al., An investment decision support tool for horticulture with an adaptive energy management system, in: 2015 6th International Conference of Information and Communication Technology for Embedded Systems (IC-ICTES), IEEE, 2015, pp. 1–6.
[119] University of Wisconsin–Madison. Solar Energy L, TRNSYS, a Transient Simulation Program, The Laboratory, Madison, Wis., 1975, 1975.
[120] A. Vadiee, V. Martin, Energy analysis and thermoeconomic assessment of the closed greenhouse – the largest commercial solar building, Appl. Energy 102 (2013) 1256–1266.
[121] A. Vadiee, M. Yaghoubi, V. Martin, et al., Energy analysis of solar blind system concept using energy system modelling, Sol. Energy 139 (2016) 297–308.
[122] L. Wang, L.K. Norford, M.J. Witte, Modeling thermal impacts of indoor living plants in the built environment, Energy Build. 346 (2025) 116113.
[123] Y. Wang, J. Du, D. Li, An investigation into PAR (Photosynthetically active radiation) and energy performances in small-scale greenhouses in Northern China, in: Proceedings of the ISES Solar World Congress 2019 and IEA SHC International Conference on Solar Heating and Cooling for Buildings and Industry 2019, 2020, pp. 1780–1790.
[124] R. Ward, R. Choudhary, C. Cundy, et al., Simulation of plants in buildings; incorporating plant-air interactions in building energy simulation, in: 14th International Conference of IBPSA-Building Simulation 2015, BS 2015, Conference Proceedings, 2015, pp. 2256–2263.
[125] D.J. Watson, Comparative physiological studies on the growth of field crops: I. Variation in net assimilation rate and leaf area between species and varieties, and within and between years, Ann. Bot. 11 (1947) 41–76.
[126] W. Yang, J. Du, D. Li, A simulation study of typical greenhouses in Beijing: PAR (Photosynthetically Active Radiation) performances and energy consumption, in: Proceedings of Building Simulation 2019: 16thConference of IBPSA, 2020, pp. 5006–5013.
[127] G. Yang, H. Shi, D. Xu, et al., Research on simulation of energy consumption of ground water-source heat pump air conditioning system in plant factory, in: IOP Conference Series: Earth and Environmental Science, IOP Publishing, 2021 012044.
[128] U.-H. Yeo, S.-Y. Lee, S.-J. Park, et al., Rooftop greenhouse: (1) design and validation of a BES model for a plastic-covered greenhouse considering the tomato crop model and natural ventilation characteristics, Agriculture 12 (2022) 903.
[129] N. Yildirim, L. Bilir, Evaluation of a hybrid system for a nearly zero energy greenhouse, Energy Convers. Manag. 148 (2017) 1278–1290.
[130] Y. Zhang, M. Kacira, Comparison of energy use efficiency of greenhouse and indoor plant factory system, Eur. J. Hortic. Sci. 85 (2020) 310–320.
[131] L. Zhang, P. Xu, J. Mao, et al., A low cost seasonal solar soil heat storage system for greenhouse heating: design and pilot study, Appl. Energy 156 (2015) 213–222.